FACTS Controllers for Grid Connected Wind Energy Conversion Systems

R. Jayashri
Department of Electrical and Electronics Engineering,
RMK Engineering College
(Affiliated with Anna University),
Kavaraipettai 601 206, TamilNadu, India
e-mail: jairavi4@yahoo.com

R. P. Kumudini Devi
Department of Electrical and Electronics Engineering,
College of Engineering,
Anna University,
Chennai 600025, India
e-mail: kumudini@annauniv.edu

In this paper, the dynamic performance of grid connected wind energy conversion system (WECS) is analyzed in terms of rotor speed stability. The WECS considered is a fixed-speed system that is equipped with a squirrel-cage induction generator. The drive-train is represented as a two-mass model. Results show that for a particular fault simulated, the voltage at the point of common coupling drops below 80% immediately after fault application and exhibits sustained oscillations. The rotor speed of induction generators becomes unstable. In order to improve the low voltage ride-through of WECS under fault conditions and to damp the rotor speed oscillations of induction generator, various flexible ac transmission system (FACTS) controllers such as static VAR (volt ampere reactive) compensator, static synchronous compensator, and unified power flow controller (UPFC) are employed. The gains of these FACTS controllers are tuned with a simple genetic algorithm. It is observed that among the FACTS controllers considered, UPFC is superior not only in regulating the voltage but also in mitigating the rotor speed instability.
[DOI: 10.1115/1.3028040]

Keywords: rotor speed stability, wind energy conversion systems, SVC, STATCOM, UPFC, squirrel-cage induction generator, fixed-speed wind turbines, genetic algorithm, point of common coupling

1 Introduction

One of the most critical issues for the development of wind energy in India has been the transmission capacity of the grid in the areas where the wind farms exist. Wind farms are concentrated in the rural areas where the existing transmission grids are very weak. In addition, the wind farms were developed during a comparatively short period of time in a few areas, and the reinforcement of the transmission systems in these areas has lagged behind the fast development of wind energy [1].

In case of fixed-speed wind turbines equipped with induction generators, reactive power support is needed at WECS terminals for voltage regulation and improvement of low voltage ride-through capabilities. As the wind speed continuously changes, the voltage at the point of common coupling (PCC) fluctuates. A possible way to improve this situation is by incorporating dynamic reactive power compensation.

When fault occurs, the voltage at the WECS terminals drops. Thus the generated active power falls, while the mechanical power does not change and so the induction generator accelerates. After fault clearance, the reactive power consumption increases, resulting in reduced voltages near the generating unit. Thus the induction generator voltage does not recover immediately after fault, but a transient period follows. As a consequence, the generator continues to accelerate, and this may lead to rotor speed instability [2]. Thus, it is clear that the dynamic controller used should not only provide the needed reactive power support for voltage regulation but should also help to damp out the rotor speed oscillations.

Many authors have discussed the application of FACTS controllers such as static var compensator (SVC) and static synchronous compensator (STATCOM) to improve the voltage ride-through of induction generators [3–12]. But the effect of these controllers in mitigating the rotor speed instability is not discussed. In this paper, the impacts of various FACTS controllers such as SVC, STATCOM, and UPFC on the stability of grid connected WECS is analyzed. Simulation results are presented for an 11-bus radial system, using the C++ programming language.

2 Dynamic Equations

Figure 1 shows the schematic of a typical WECS. The dynamic equations include the differential and algebraic equations pertaining to the models of wind turbine, the mechanical model of the drive-train, induction generator, and the power system. These are described in the following sections.

2.1 Wind Turbine Model. The simple aerodynamic model commonly used to represent the turbine is based on power performance versus tip-speed ratio. The power extracted from the wind turbine is given by [13]

$$P_w = \tfrac{1}{2}\rho A C_P v^3 \tag{1}$$

where ρ is the density of dry air, v is the velocity of the wind in m/s, A is the swept area of the blades in m^2, and C_P is the power coefficient. A general expression for C_P is given in Ref. [14].

2.2 Drive-Train Model. In the case of a conventional WECS model, accurate results are obtained by increasing the number of masses, springs, and damper, which are used to represent the physical characteristics of the actual system. It has been proved that the two-mass model for WECS representation is fairly accurate [5]. Thus this approach is adopted here and is shown in Fig. 2. As shown in Fig. 2, the wind turbine and the generator rotor are modeled as two masses and the wind mill shafts as a spring element.

The dynamic equations of the two-mass representation is given by [15]

Contributed by the Solar Energy Engineering Committee of ASME for publication in the JOURNAL OF SOLAR ENERGY ENGINEERING. Manuscript received November 14, 2007; final manuscript received June 1, 2008; published online January 7, 2009. Review conducted by Spyros Voutsinas.

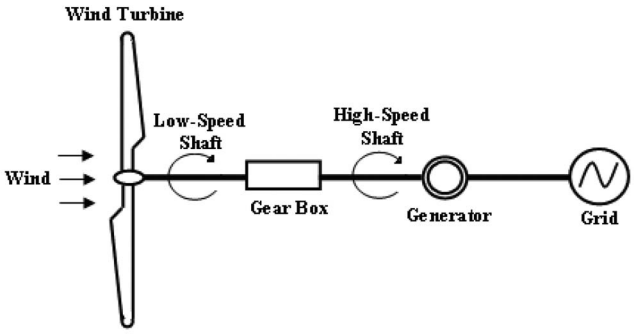

Fig. 1 Schematic of a typical WECS

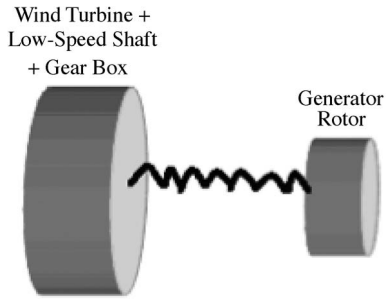

Fig. 2 The simplified two-mass model

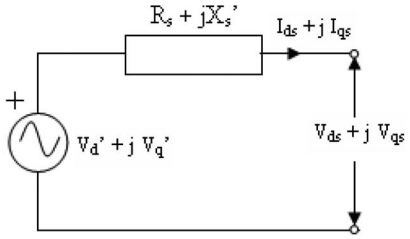

Fig. 3 Induction generator transient model

$$\frac{d\omega_t}{dt} = \frac{T_t - K_s\delta}{2H_t}$$

$$\frac{d\omega_e}{dt} = \frac{K_s\delta - T_e}{2H_e}$$

$$\frac{d\delta}{dt} = 2\pi f(\omega_t - \omega_e) \tag{2}$$

where T is the torque, δ is the angular displacement between the two ends of the shaft, ω is the angular speed, H is the inertia constant, and K_s is shaft stiffness. The indices t and e stand for wind turbine and generator, respectively.

2.3 Electric Generator. The induction generator is represented by the well known third order model [16]. The stator flux linkage transients are neglected, so that only fundamental frequency components are represented. This results in the Thevenin equivalent circuit shown in Fig. 3.

The differential equations are then given by

$$\frac{dV'_d}{dt} = -\frac{1}{T'_0}[V'_d + (X_s - X'_s)I_{qs}] + sV'_q$$

$$\frac{dV'_q}{dt} = -\frac{1}{T'_0}[V'_q - (X_s - X'_s)I_{ds}] - sV'_d \tag{3}$$

where V' is the voltage behind transient reactance, I_s is the stator current, s is the slip, T'_0 is the open circuit time constant, and X'_s is the transient reactance of the machine. The subscripts d and q stand for the direct and quadrature axis values, respectively.

The third differential equation is the swing equation, which has been included in the mechanical model. The electromagnetic torque is computed as

$$T_e = V'_d I_{ds} + V'_q I_{qs} \tag{4}$$

where T_e is the electromagnetic torque.

3 Description of the System Considered

An 11-bus radial system is considered for analysis. It consists of a wind farm with ten wind turbines, each rated at 750 kW and is shown in Fig. 4. Fixed capacitors with 150 kVAR (kilo volt ampere reactive) rating is connected at the terminals of each wind turbine. At the PCC, the wind turbines are connected in two groups: Group 1 consisting of three turbines, connected at bus 10, and Group 2 consisting of seven turbines, connected at bus 11. The distance between the wind turbines in each group is taken as 500 m. The feeder between the wind farm and grid is a 10 km

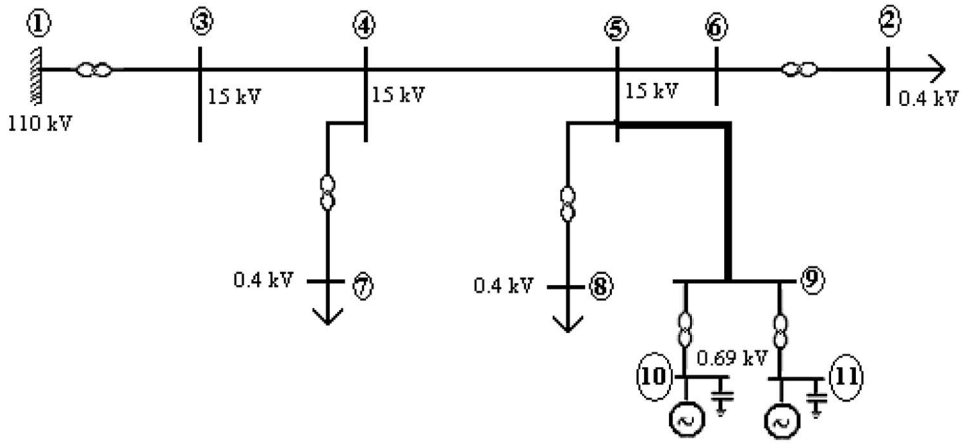

Fig. 4 Single line diagram of the 11-bus radial system

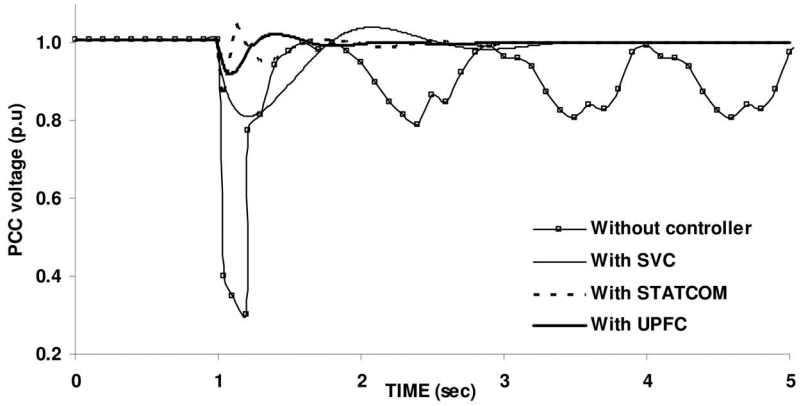

Fig. 5 PCC voltage for a solid three-phase to ground fault of Case 1

double circuit line. The data for the system are given in the Appendix. In this paper, the investigations are executed on the assumption that all the wind turbines in the wind farm are identical and have the same operating condition. Thus, the three turbines of Group 1 are aggregated together as one single turbine of a capacity of 2.25 MW (750 kW × 3) connected at bus 10. Similarly, the seven turbines of Group 2 are aggregated together as one single turbine of a capacity of 5.25 MW (750 kW × 7) connected at bus 11.

4 Rotor Speed Stability Analysis

The rotor speed stability analysis is carried out by evaluating the transient stability of the system. The initial steady state values of powers (P,Q), magnitude, and phase angles of the voltages at all buses and the operating value of slip of the induction generator are obtained by a simultaneous method of power flow analysis [17]. The time response of rotor speed of the induction generators and the PCC voltage are obtained for the following case.

Case 1. A solid three-phase to ground fault on one of the interconnecting lines between the wind farm PCC (bus 9) and the grid (bus 5) near bus 9 at 1 s followed by tripping of faulted line between buses 9 and 5 after a delay of 5 cycles when the WECS is operating at rated speed (17 m/s).

Figures 5 and 6 show the voltage at the PCC and the rotor speed of WECS. It is seen that without any controller, the PCC voltage drops to a very low value of 0.31 p.u. (per unit) initially and does not settle down. It exhibits sustained oscillations. In Fig. 6, it is seen that the amplitude of speed oscillations of the induction generators increases with time, which indicates clear rotor speed instability.

5 Impact of FACTS Controllers

The power generation by the WECS depends on the wind speed. Figure 7 gives the reactive power absorbed by the induction generator (data given in the Appendix) with changes in wind speed. It can be observed that the reactive power demand varies continuously with the variation in wind speed. It can also be seen that the induction generator absorbs about 150–300 kVAR from the grid when wind speed varies from cut-in (5 m/s) to cut-out (25 m/s) speed. So connecting fixed capacitor for reactive power compensation will not yield better performance.

In this paper, a fixed capacitor equal to the no-load (operation at cut-in speed) compensation of 150 kVAR is assumed to be connected at the terminals of each generator. Then, the dynamic VAR requirement at the PCC that has to be supplied by FACTS controllers is selected as the difference between full-load (operation at rated speed) and no-load compensations. Thus the rating of the FACTS controllers is set to ±1.5 MVAR (150 kVAR × 10), capacitive.

The gains of the controllers are tuned by using a simple genetic algorithm (GA) [18]. GA is a computerized search and optimization algorithm based on the mechanics of natural genetics and natural selection. In this paper, GA is chosen for tuning of controller gains as it helps to achieve global optimum, while the conventional optimization methods may end up in local optimum.

GA works on a set of population of the problem variables coded in some string structures. The population is a group of binary strings, consisting of a number of binary substrings. The number of substrings is equal to the number of gains of the controller that has to be tuned. Each binary substring represents the feasible value for each parameter of interest. The length of the string de-

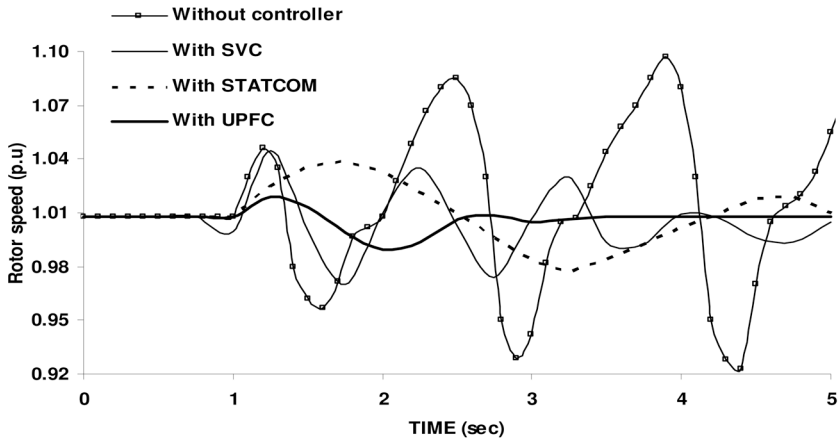

Fig. 6 Rotor speed of WECS for a solid three-phase to ground fault of Case 1

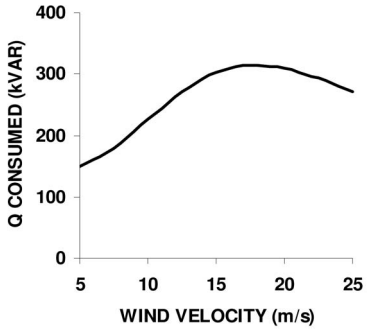

Fig. 7 *Q* variation of a single wind turbine

pends on the accuracy desired. The equivalent decimal value of the variable in the search space is found using some linear mapping rule. GAs mimic the survival of the fittest principle of nature to make a search process. Therefore, a fitness function is derived from the objective function and is used in successive genetic operations. The population is generated randomly, and thereafter each string is evaluated to find the fitness value, called the string fitness. The member with the higher value of the fitness will have more opportunities to pass on genetically important information to successive generations. The population is then operated by three main operators, namely, reproduction, crossover, and mutation. The new population is further evaluated and tested for termination. This iterative process is continued until a termination criterion is met.

In this paper, the tuning of controller gains is posed as an optimization problem with the sum squared deviation index (SSDI) of the PCC voltage as the objective function. SSDI is given by

$$\text{SSDI} = \sum_{k} (V_{\text{ref}} - V_k)^2 \tag{5}$$

where $V_{\text{ref}}=1.0$ p.u., V_k is the PCC voltage.

5.1 Simulation With SVC. SVC is a shunt connected static generator and/or absorber of reactive power whose output is varied so as to control specific parameters of the electric power system. From the viewpoint of power system operation, a SVC is equivalent to a parallel combination of a shunt capacitor and a shunt inductor, both of which can be adjusted using a thyristor switch to control voltage and reactive power at the bus to which they are connected. With the use of SVC, the reactive power can be varied steplessly.

In this paper, the SVC considered is of a fixed capacitor +thyristor controlled reactor (FC+TCR) configuration with a simple gain-time constant model, as shown in Fig. 8.

From Fig. 8, the state equation for SVC can be written as

$$\dot{B}_{\text{SVC}} = \frac{K}{T}(V_{\text{ref}} - V_{\text{meas}}) - \frac{1}{T}B_{\text{SVC}} \tag{6}$$

Here, V_{meas} is the PCC voltage.

For the 11-bus system in Fig. 4, simulation is carried out with SVC with rating of 1.5 MVAR (capacitive) at the PCC along with 150 kVAR FC at each of the generator terminals. The gain K of SVC is initially chosen as 10. The time constant T of the SVC is selected as 0.01 s. After tuning with GA, the SSDI is reduced from 0.3811 to 0.2679, and the optimum gain of the SVC is obtained as 2.8361. With this tuned gain of 2.8361, simulation is carried out for the three-phase fault described in Case 1 with SVC connected at the PCC (bus 9). Figure 5 shows that the PCC voltage settles within 2.34 s with SVC. The initial transient dip in voltage is improved to 0.81 p.u. Figure 6 shows that although the rotor speed oscillations get damped, they do not settle down quickly.

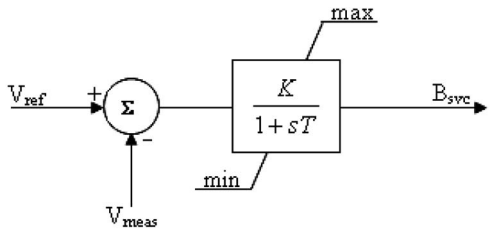

Fig. 8 SVC model

5.2 Simulation With STATCOM. STATCOM is a shunt connected device that is capable of generating and/or absorbing reactive power and in which the output can be varied to control the specific parameters of an electric power system. It is basically a voltage source converter that produces a set of three-phase ac voltages from the dc voltage. The dc voltage is provided by an energy storage capacitor.

The transient model of STATCOM is adopted from Canizares et al. [19]. The model is based on the power balance technique, which basically represents the balance between the controller's ac power and dc power under balanced operation at fundamental frequency. The shunt controller of the STATCOM consists of a pulse width modulation (PWM) based voltage magnitude controller and a proportional-integral (PI) based phase angle controller. The transfer function of the voltage magnitude controller is given by

$$G(s) = \frac{K(1 + sT_1)}{K_D + sT_2} \tag{7}$$

and the transfer function of the phase angle controller is given by

$$G(s) = K_P + \frac{K_I}{s} \tag{8}$$

Thus, the STATCOM is represented as a fifth order model.

The rating of the STATCOM connected at the PCC is chosen as ± 1.5 MVAR. For the 11-bus system shown in Fig. 4, simulation is carried out with STATCOM connected at the PCC along with 150 kVAR FC at each of the generator terminals. The initial value of the gains K, K_D, and K_P are chosen as 10, and K_I is chosen as 1. The time constants T_1 and T_2 are selected as 1.0 s and 0.01 s, respectively. Using GA, all four gains are simultaneously tuned. After tuning it is observed that the SSDI is reduced from 0.2379 to 0.1263. The optimum gain values are obtained as $K=7.3463$, $K_D=9.8632$, $K_P=6.5823$, and $K_I=0.5447$.

With these optimum gains, simulation is carried out for the Case 1 fault. Figures 5 and 6 show that with STATCOM, the oscillations in both voltage and speed are less. The voltage oscillations get damped out in 1.91 s. The initial transient voltage is better with STATCOM and is equal to 0.87 p.u. Similarly, the rotor speed oscillations settle down in 5.76 s with STATCOM, and with SVC the speed oscillations settle down in 8.01 s.

5.3 System Response With UPFC. From the above analysis, it is seen that the STATCOM improves the low voltage ride-through of induction generators better than SVC. However, the damping of speed oscillations is not very much improved either with SVC or STATCOM. Therefore, for improving both the rotor speed stability and voltage ride-through of WECS, a dynamic controller that incorporates a series compensator along with shunt compensation is necessary. Such a type of controller is UPFC, which can independently control both the real and reactive flows in a line.

UPFC is a shunt-series-connected FACTS controller that can control the various electrical parameters (voltage, real power, and reactive power) either individually or simultaneously. The transient model of UPFC is adopted from Canizares et al. [20]. The power balance equation couples the shunt and series ac/dc converters through its common dc link. The shunt controller of UPFC

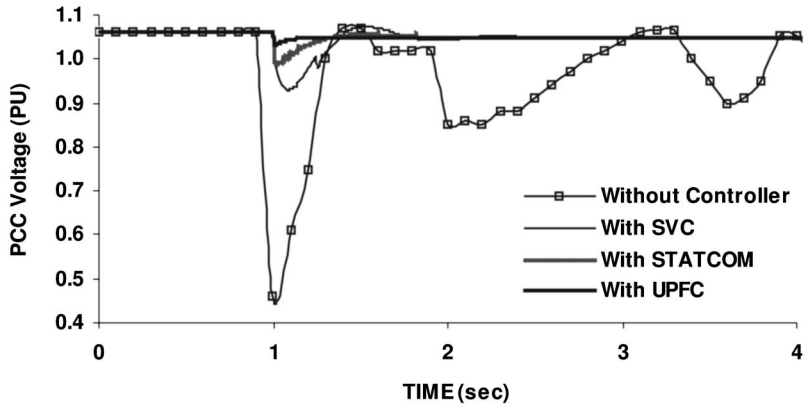

Fig. 9 PCC voltage for the Case 2 fault

is similar to that of the STATCOM model described in Sec. 5.2. Thus, the transfer functions given in Eqs. (7) and (8) apply to the UPFC shunt controller also.

The series controller is used to control power flows on the transmission line by regulating the magnitude and phase angle of the series injected voltage. The transfer function of the series voltage controller is given by

$$G(s) = K_{P_P} + \frac{K_{I_P}}{s} \tag{9}$$

and the transfer function of the series phase angle controller is given by

$$G(s) = K_{P_Q} + \frac{K_{I_Q}}{s} \tag{10}$$

Thus, the UPFC is represented as a ninth order model.

As the UPFC consists of both shunt and series controllers, the objective of GA tuning is redefined as minimizing the oscillations in PCC voltage and rotor speed. Thus the SSDI for tuning the gains of UPFC may be written as

$$\text{SSDI} = \sum_k [(V_{\text{ref}} - V_k)^2 + (\omega_{\text{ref}} - \omega_k)^2] \tag{11}$$

The initial values of the shunt controller gains are the same as those chosen for STATCOM. The initial values of the series controller gains K_{PP} and K_{PQ} are chosen as 10 and K_{IP} and K_{IQ} are chosen as 1.0. Using GA, all eight gains are simultaneously tuned. After tuning it is observed that the SSDI is reduced from 0.1124 to 0.0347. The optimum gain values are obtained as K=7.6932, K_D=9.7652, K_P=6.4625, K_I=0.4369, K_{PP}=2.6936, K_{IP}=0.0498, K_{PQ}=5.2894, and K_{IQ}=0.3836.

With these optimum gains, simulation is carried out for the Case 1 fault with UPFC of rating ±1.5 MVA connected between buses 9 and 5 along with 150 kVAR FC at each of the generator terminals. Figures 5 and 6 show that with UPFC, the oscillations in both voltage and speed are minimum. It is observed that the PCC voltage oscillations get damped out in 1.7 s and the rotor speed oscillations take 2.52 s to settle down. It is also seen that the initial transient voltage dip decreases by 0.06 p.u. with UPFC as compared to STATCOM.

6 Effects of Tuned FACTS Controllers for Other Faults

To examine the effects of the above controllers for other faults, the following fault is simulated as Case 2.

Case 2. A solid three-phase to ground fault at the terminals of Group 2 machines (seven machine group, connected at bus 11) when operating at full-load (17 m/s) for 1 s. The fault is cleared after a delay of 5 cycles, followed by tripping of all seven induction generators connected at bus 11.

Figures 9 and 10 give the PCC voltage and rotor speed oscillations of Group 1 machines with and without FACTS controllers for Case 2. Figure 9 shows that immediately after fault, the PCC voltage drops to a low value of 0.41 p.u. without controller. However, the voltage recovers and settles down to the original value. Figure 10 shows the oscillations on the generator speed of Group 1 machines. The oscillations are of very high amplitude initially and take around 8 s to settle down. With SVC, the PCC voltage settles in 1.4 s. However, the rotor speed oscillations do not settle down that quickly. With STATCOM the oscillations in both volt-

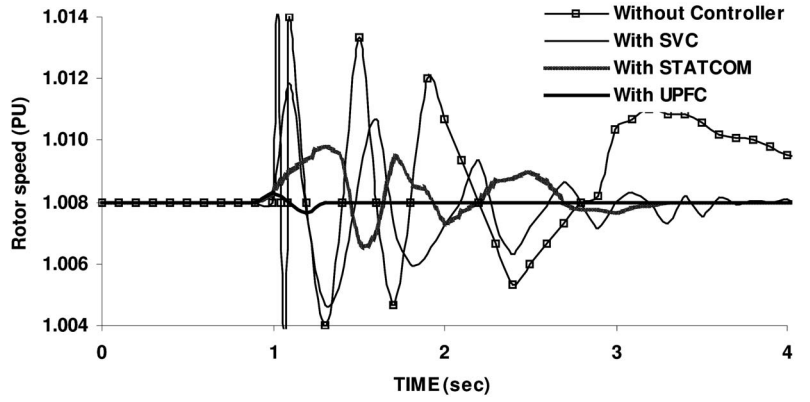

Fig. 10 Rotor speed oscillations of Group 1 machines for the Case 2 fault

Table 1 Comparison between SVC, STATCOM, and UPFC

	Case 1			Case 2		
		Settling time (s)			Settling time (s)	
Type of controller	Initial transient voltage (p.u.)	PCC voltage	Rotor speed	Initial transient voltage (p.u.)	PCC voltage	Rotor speed
No controller	0.31	Diverging	Diverging	0.41	8.01	8.01
SVC	0.81	2.34	8.01	0.88	1.41	3.71
STATCOM	0.87	1.91	5.76	0.94	0.96	2.29
UPFC	0.93	1.70	2.52	0.98	0.33	0.40

age and speed are less. The voltage oscillations get damped out in 0.98 s. The initial transient voltage with STATCOM is 0.94 p.u., whereas with SVC it is 0.88 p.u. Similarly, the rotor speed oscillations settle in 2.3 s with STATCOM, and with SVC speed oscillations settle down in 3.7 s. As observed from Fig. 10, the amplitude of rotor speed oscillations is decreased with STATCOM. With UPFC, the oscillations in both voltage and speed are minimum. Voltage settles down in 0.33 s and rotor speed oscillations take around 0.4 s to damp out. It is also seen that the initial transient voltage with UPFC is 0.98 p.u. Thus the low voltage ride-through is highly improved with UPFC.

7 Conclusion

Almost without exception, wind farms require VAR management. After exploring various VAR management techniques, it is found that wind farms operate under unique conditions, and the traditional VAR management by capacitor banks has an adverse impact. Employing dynamic VAR devices, sometimes in combination with and in control of capacitor banks, eliminates the negative consequences of the traditional solution. In this paper, the effects of dynamic compensators, namely, SVC, STATCOM, and UPFC, on improving the rotor speed stability and voltage ride-through of WECS are analyzed. The gains of the controllers are tuned with a simple GA. It is clear that the magnitude and frequency of oscillations are reduced appreciably after tuning the controller gains with GA.

Table 1 gives the comparison between the various controllers for solid three-phase faults as described in Cases 1 and 2. From the results presented in Table 1, it is clear that the settling time in both PCC voltage and rotor speed and the initial transient dip in voltage are lesser with UPFC than with SVC or STATCOM. Thus it is concluded that dynamic compensation with a 150 kVAR fixed capacitor at the generator terminals and ± 1.5 MVA UPFC between the PCC and bus 5 provides the best solution for the 11-bus system, among the controllers considered.

The study reveals that in certain cases, adequate VAR compensation can be achieved by using the existing capacitor banks along with the FACTS controllers. This way the rating of the FACTS controllers can be reduced. This will lead to a considerable reduction in economy, as the FACTS controllers are very expensive. Moreover, total dispensing of the existing capacitor banks can be avoided.

Appendix

Transmission line data (all lines). Resistance: 0.19 Ω/km; reactance: 0.24 Ω/km, susceptance: 2.80 μs/km; and Length: 20.0 km.

Asynchronous generator data. (Δ-*connection*) Stator resistance: 0.0034 Ω; Rotor resistance: 0.003 Ω; stator leakage reactance: 0.055 Ω, rotor leakage reactance: 0.042 Ω, magnetizing reactance: 1.6 Ω, rotor inertia: 5 sec; generator inertia: 0.45 sec, shaft stiffness: 50 p.u., and shaft damping coefficient: 1 p.u.

Load transformer data. Rated apparent power: 0.63 MVA, nominal short-circuit voltage: 6%, and copper loss at rated power: 6 kW.

Step-up transformer data. Rated apparent power: 1 MVA, nominal short-circuit voltage: 6%, and copper loss at rated power: 13.58 kW.

Feeding transformer data. Rated apparent power: 25 MVA, nominal short-circuit voltage: 11%, and copper loss at rated power: 110 kW.

Load data (all loads): 0.150+j0.147 MVA

Nomenclature

T_0' = open circuit time constant
X_s' = transient reactance of the machine
δ = angular displacement between the two ends of the shaft
ω = angular speed
ρ = density of dry air
A = swept area of the blades (m^2)
C_P = power coefficient
H = inertia constant
I_s = stator current
K_s = shaft stiffness
R_s = stator resistance
s = slip
T = torque
T_e = electromagnetic torque
v = velocity of the wind in m/s
V = terminal voltage of induction generator
V' = voltage behind transient reactance

References

[1] Yao, L., Cartwright, P., Schmitt, L., and Zhang, X.-P., 2005, "Congestion Management of Transmission Systems Using FACTS," *IEEE/PES Transmission and Distribution Conference and Exhibition: Asia and Pacific*, Dalian, China, pp. 1–5.

[2] Samuelsson, O., 2005, "On Speed Stability," IEEE Trans. Power Syst., **20**(2), pp. 1179–1180.

[3] Saad-Saoud, Z., and Jenkins, N., 1997, "The Application of Advanced Static VAr Compensators to Wind Farms," *IEE Colloquium on Power Electronics for Renewable Energy*, London, June.

[4] Ezzeldin, S. A., and Xu, W., 2000, "Control Design and Dynamic Performance Analysis of a Wind Turbine: Induction Generator Unit," IEEE Trans. Energy Convers., **15**(1), pp. 91–96.

[5] Akhmatov, V., Knudsen, H., Nielsen, A. H. Pedersen, J. K., and Poulsen, N. K., 2003, "Modelling and Transient Stability of Large Wind Farms," Int. J. Electr. Power Energy Syst., **25**(2), pp. 123–144.

[6] Ahmed, T., Noro, O., Hiraki, E., and Nakaoka, M., 2004, "Terminal Voltage Regulation Characteristics by Static Var Compensator for a Three-Phase Self-Excited Induction Generator," IEEE Trans. Ind. Appl., **40**(4), pp. 978–988.

[7] Chompoo-inwai, C., Yingvivatanapong, C., Methaprayoon, K., and Lee, W.-J., 2005, "Reactive Compensation Techniques to Improve the Ride-Through of Induction Generators During Disturbance," IEEE Trans. Ind. Appl., **41**(3), pp. 666–672.

[8] Saad-Saoud, Z., Lisboa, M. L., Ekanayake, J. B., Jenkins, N., and Strbac, G., 1998, "Application of STATCOMs to Wind Farms," IEE Proc.: Gener. Transm. Distrib., **145**(5), pp. 511–516.

[9] Molinas, M., Vazquez, S., Takaku, T., Carrasco, J. M., Shimada, R., and Un-

deland, T., 2005, "Improvement of Transient Stability Margin in Power Systems With Integrated Wind Generation Using a STATCOM: An Experimental Verification," *Proceedings of the Future Power Systems Conference*, Amsterdam, November.
[10] Han, C., Huang, A. Q., Litzenberger, W., Anderson, L., Edris, A.-A., Baran, M., Bhattacharya, S., and Johnson, A., 2006, "STATCOM Impact Study on the Integration of a Large Wind Farm into a Weak Loop Power System," *IEEE PSCE*, Atlanta, October, pp. 1266–1272.
[11] Banos, C., Aten, M., Cartwright, P., and Green, T. C., 2006, "Benefits and Control of STATCOM with Energy Storage in Wind Power Generation," *8th IEE International Conference on ACDC*, London, UK, March, pp. 230–235.
[12] Gaztanaga, H., Etxeberria-Otadui, I., Ocnasu, D., and Bacha, S., 2007, "Real-Time Analysis of the Transient Response Improvement of Fixed-Speed Wind Farms by using a Reduced-Scale STATCOM Prototype," IEEE Trans. Power Syst., **22**(2), pp. 658–666.
[13] Lubosny, A., 2003, *Wind Turbine Operation in Electric Power Systems: Advanced Modelling*, Springer, New York.
[14] Heier, S., 1998, *Grid Integration of Wind Energy Conversion Systems*, Wiley, New York.
[15] Slootweg, J. G., Polinder, H., and Kling, W. L., 2003, "Representing Wind Turbine Electrical Generating Systems in Fundamental Frequency Simulations," IEEE Trans. Energy Convers., **18**(4), pp. 516–524.
[16] Kundur, P., 1994, *Power System Stability and Control*, McGraw-Hill, New York.
[17] Jayashri, R., and Kumudini Devi, R. P., 2006, "Analysis of the Impact of Interconnecting Wind Turbine Generators to the Utility Grid," Wind Eng., **30**(4), pp. 303–315.
[18] Goldberg, D. E., 1989, *Genetic Algorithms in Search, Optimization and Machine Learning*, Addison-Wesley, Reading, MA.
[19] Canizares, C. A., Pozzi, M., Corsi, S., and Uzunovic, E., 2003, "STATCOM Modeling for Voltage and Angle Stability Studies," Int. J. Electr. Power Energy Syst., **25**(6), pp. 431–441.
[20] Canizares, C. A., Uzunovic, E., and Reeve, J., 2004, "Transient Stability and Power Flow Models of the Unified Power Flow Controller for Various Control Strategies," University of Waterloo, Technical Report.